Radiation-Induced Creep in Single Crystals of Face-Centered Cubic Materials

W.G. Wolfer

October 1979

UWFDM-326

Phil. Mag. A31, 61-70 (1981).

FUSION TECHNOLOGY INSTITUTE

UNIVERSITY OF WISCONSIN

MADISON WISCONSIN

Radiation-Induced Creep in Single Crystals of Face-Centered Cubic Materials

W.G. Wolfer

Fusion Technology Institute
University of Wisconsin
1500 Engineering Drive
Madison, WI 53706

http://fti.neep.wisc.edu

October 1979

UWFDM-326

Phil. Mag. A31, 61-70 (1981).

RADIATION-INDUCED CREEP IN SINGLE CRYSTALS OF FACE-CENTERED CUBIC MATERIALS

by

W.G. Wolfer
University of Wisconsin
Madison, Wisconsin 53706 U.S.A.

October 1979

UWFDM-326

Abstract

In order to find the dislocation mechanisms responsible for radiation-induced creep, experiments on single crystals are proposed. Three possible mechanisms are considered: stress-induced preferential absorption of interstitials at Frank loops (SIPAL), or at edge dislocations (SIPAD), and climb-controlled glide of dislocations (CCG).

The dependence of radiation-induced creep on the single crystal orientation is derived for face-centered cubic materials. It is shown that each mechanism gives rise to a distinct orientation dependence, and specific examples are worked out for uniaxial tension and for torsion of bar specimens. In addition, we discuss briefly the significance of single crystal irradiation creep to polycrystalline behavior.

§1. INTRODUCTION

Radiation-induced creep of non-fissile cubic metals has become the subject of a growing experimental effort in recent years in connection with the development of nuclear breeder reactors (Harris 1977, Gilbert et al., 1977). As a consequence, this has also spurred the interest in the physical basis of this phenomenon, and several mechanisms have been proposed. Among these, the stress-induced preferential absorption (SIPA) of interstitials at dislocations has been discovered recently (Heald and Speight 1974, Wolfer et al., 1976, Wolfer and Ashkin 1976) as a viable mechanism for irradiation creep, whereas mechanisms based on dislocation glide have been considered in many variations over the years.

The SIPA mechanism produces the creep deformation through the climb of dislocations and the growth of dislocation loops, and it yields in a natural way a linear stress dependence of the creep rate. In contrast, models based on dislocation glide exhibit various stress-dependencies, including linear, according to the specific assumptions made on the nature of the glide obstacles (Wolfer and Boltax 1973). The experimental evidence clearly favors the linear stress dependence, although non-linear relationships have occasionally been reported.

In order to elucidate further the mechanistic aspects of irradiation creep, it appears that experiments on single crystals offer great promise. Accordingly, it is the major goal of this paper to present the irradiation-creep relationships for face-centered cubic (fcc) single crystals as based on three mechanisms: SIPA for faulted dislocation loops, SIPA for edge dislocations (or unfaulted loops), and climb-controlled glide (CCG). The

results to be reported show that each mechanism gives a different dependence of the irradiation creep rate on the crystalline orientation, and consequently, measurements on single crystals should reveal to what extent each mechanism contributes to the deformation.

Apart from the basic interest in this question, it may also be of practical importance. We name two examples. It has recently been demonstrated (Bloom and Wolfer 1978) that irradiation creep has a beneficial effect on creep rupture times, presumably because the deformation within the grain diminishes grain boundary sliding and the concurrent formation of grain boundary cavities. For this to be effective, the irradiation creep properties should not vary drastically from grain to grain. This requirement is not satisfied if faulted loops contribute predominantly to irradiation creep. It appears that some alloys under development for greater swelling resistance do evolve under irradiation a dislocation structure dominated by faulted loops. Based on the above arguments, these alloys are expected to develop adverse ductility properties.

Another consequence of the effect of crystal orientation on irradiation creep has been investigated recently (Wolfer 1978). It was shown that when grain to grain variations exist for irradiation creep, a polycrystal exhibits anelastic effects upon load changes. Hence, upon load removal, some of the irradiation creep strain recovers if the irradiation is continued.

§2. STRAIN RATE TENSOR DUE TO CLIMB

The dislocation structure of fcc metals irradiated at reactor temperatures consists of faulted interstitial loops, perfect interstitial loops,

and network dislocations. The latter two have <110> Burgers vectors, whereas the former possess <111> Burgers vectors. With regard to climb, we can treat the edge components of both perfect loops and network dislocations as one type of sink, henceforth simply called edge dislocations. We label the 12 possible Burgers vectors of edge dislocations in an fcc lattice by a superscript m, i.e., by $\underset{\sim}{b}^m$. Similarly, the four possible Burgers vectors of faulted loops are denoted by $\underset{\sim}{b}^n$.

The preferential absorption of point defects at both edge dislocations and faulted loops causes climb, which in turn results in a macroscopic strain rate expressed by

$$\dot{\varepsilon}_{ij} = \Omega \sum_{n=1}^{4} N_n \left(J_I^n - J_V^n\right) \hat{b}_i^n \hat{b}_j^n + \Omega \sum_{m=1}^{12} \rho_m \int d\omega_{\underset{\sim}{\ell}} \, \delta\left(\hat{\underset{\sim}{\ell}} \cdot \hat{\underset{\sim}{b}}^m\right) \left(J_I^m - J_V^m\right) \hat{b}_i^m \hat{b}_j^m \quad . \tag{13}$$

Here, Ω is the atomic volume, N_n the number per unit volume of loops with Burgers vector $\underset{\sim}{b}^n$, and J_I^n and J_V^n are the currents of interstitials and vacancies to one loop. Similarly, in the second term, ρ_m is the edge dislocation density with Burgers vector $\underset{\sim}{b}^m$, and $J_{I,V}^m$ are point defect currents per unit length of the dislocation. With regard to the line direction $\hat{\underset{\sim}{\ell}}$ of the edge dislocation, it is assumed that all directions occur with equal probability. Since $\hat{\underset{\sim}{\ell}}$ must be perpendicular to $\hat{\underset{\sim}{b}}^m$, the integration over all directions of $\hat{\underset{\sim}{\ell}}$ is restricted as expressed by the δ-function in the second term.

The net flow of atoms to a dislocation loop is given by

$$J_I^n - J_V^n = 4\pi R[Z_I^{\ell} D_I C_I - Z_V^{\ell} D_V C_V + Z_V^{\ell} D_V C_V^n] \quad . \tag{14}$$

The similar expression

$$J_I^m - J_V^m = \frac{2\pi}{\ell n(d/a)} [Z_I^d D_I C_I - Z_V^d D_V C_V + Z_V^d D_V C_V^m] \tag{15}$$

gives the net flow of atoms per unit length of an edge dislocation.

Here, C_V and C_I are the average concentrations of vacancies and interstitials, respectively, and D_V and D_I the corresponding diffusion coefficients. R is the loop radius, 2d the average distance between dislocations, and a is the core radius.

The vacancy concentrations in equilibrium with loops, C_V^n, and edge dislocations, C_V^m, depend on the stress and the orientation of the corresponding Burgers vector by a factor

$$\exp\{\hat{b}_i \tilde{\sigma}_{ij} \hat{b}_j \Omega/kT\} \cong 1 + \frac{\Omega}{kT} \hat{b}_i \tilde{\sigma}_{ij} \hat{b}_j \tag{16}$$

where $$\tilde{\sigma}_{ij} = \sigma_{ij} - \frac{1}{3} \delta_{ij} \sigma_{kk} \tag{17}$$

is the deviatoric stress tensor, and repeated indices indicate a summation. As indicated in Eq. (14), a linear expansion in the stress suffices for the following analysis since $\sigma\Omega/kT << 1$ for all practical purposes.

The bias factors for both loops, Z^{ℓ}, and edge dislocations, Z^d, are functions of the deviatoric stresses. According to perturbation theoretical calculations (Wolfer and Ashkin, 1975, 1976) these bias factors can be written as

$$Z^{\ell} = Z^{\ell}(o) + \delta Z^{\ell}(\tilde{\sigma}) = Z^{\ell}(o) + \zeta^{\ell}\hat{b}_i\hat{b}_j\tilde{\sigma}_{ij} \tag{18}$$

and

$$Z^{d} = Z^{d}(o) + \delta Z^{d}(\sigma_{kk}) + \delta Z^{d}(\tilde{\sigma})$$

$$= Z^{d}(o) + \delta Z^{d}(\sigma_{kk}) + \zeta^{d}[2\hat{b}_i\hat{b}_j - (1-4\nu)\hat{\ell}_i\hat{\ell}_j]\tilde{\sigma}_{ij} \quad , \tag{19}$$

where ν is Poisson's ratio.

The stress-free bias factors $Z^{\ell}(o)$ and $Z^{d}(o)$, the term $\delta Z^{d}(\sigma_{kk})$ induced by the hydrostatic stress, and the parameters ζ^{ℓ} and ζ^{d} were derived previously (Wolfer and Ashkin, 1975 and 1976), and they need not be specified explicitly for the present purpose.

If we insert now the expressions for the bias factors, Eqs. (18) and (19), and the stress dependence factor for C_V^n and C_v^m, Eq. (16), into Eq. (13), we find that the total strain rate tensor can be written as a sum of three terms,

$$\dot{\varepsilon}_{ij} = \dot{S}_{ij} + \dot{e}_{ij}^{IC} + \dot{e}_{ij}^{TC} \quad . \tag{20}$$

Here, $\dot{S}_{ij}$ is the irradiation growth rate tensor, $\dot{e}_{ij}^{IC}$ the irradiation creep tensor, and $\dot{e}_{ij}^{TC}$ the thermal creep tensor.

This interpretation is suggested by the definitions for

$$\dot{S}_{ij} = \Omega \sum_{n=1}^{4} N_n 4\pi R_n \{Z_I^{\ell}(o)D_I C_I - Z_V^{\ell}(o)D_V(C_V - C_V^{\ell})\}\hat{b}_i^n\hat{b}_j^n$$

$$+ \frac{2\pi}{\ell n(d/a)} \sum_{m=1}^{12} \rho_m \int d\omega_{\ell}\delta(\hat{\underset{\sim}{\ell}}\cdot\hat{\underset{\sim}{b}}^m)\{[Z_I^{d}(o) + \delta Z_I^{d}(\sigma_{kk})]\, D_I C_I \tag{21}$$

$$- [Z_V^{d}(o) + \delta Z_I^{d}(\sigma_{kk})]D_V(C_v - C_V^{d})\}\hat{b}_i^m\hat{b}_j^m$$

which is independent of the deviatoric stress, but does contain terms dependent on the hydrostatic stress σ_{kk}. On the other hand, both creep tensors, $\dot{e}_{ij}^{IC}$ and $\dot{e}_{ij}^{TC}$, are linear in the deviatoric stress. A distinction between these two contributions to the total strain rate can be made uniquely by the requirement that $\dot{e}_{ij}^{TC}$ be independent of the radiation-enhanced point defect concentrations C_V and C_I. This leads to the definition for the thermal creep rate tensor

$$\dot{e}_{ij}^{TC} = \Omega \sum_{n=1}^{4} N_n 4\pi R_n Z_V^{\ell}(o)\, D_V C_V^{\ell} \frac{\Omega}{kT}\, \tilde{\sigma}_{k\ell}\, \hat{b}_k^n \hat{b}_\ell^n \hat{b}_i^n \hat{b}_j^n \tag{22}$$

$$+ \frac{2\pi}{\ell n(d/a)} \sum_{m=1}^{12} \rho_m \int d\omega_{\ell}\, \delta(\hat{\underset{\sim}{\ell}} \cdot \hat{\underset{\sim}{b}}^m)\, D_V C_V^{d} \frac{\Omega}{kT}\, \tilde{\sigma}_{k\ell}\, \hat{b}_k^m \hat{b}_\ell^m \hat{b}_i^m \hat{b}_j^m$$

which is a generalization of the Nabarro creep mechanism (Nabarro 1967).

The irradiation creep rate tensor is then the remainder, and it is given by

$$\dot{e}_{ij}^{IC} = \Omega \sum_{n=1}^{4} N_n 4\pi R_n \{\delta Z_I^{\ell}(\tilde{\sigma}) D_I C_I - \delta Z_V^{\ell}(\tilde{\sigma}) D_V [C_V - C_V^{\ell}]\} \hat{b}_i^n \hat{b}_j^n$$

$$+ \frac{2\pi}{\ell n(d/a)} \sum_{m=1}^{12} \rho_m \int d\omega_{\ell}\, \delta(\hat{\underset{\sim}{\ell}} \cdot \hat{\underset{\sim}{b}}^m) \{\delta Z_I^{d}(\tilde{\sigma})\, D_I C_I \tag{23}$$

$$- \delta Z_V^{d}(\tilde{\sigma})\, D_V [C_V - C_V^{d}]\} \hat{b}_i^m \hat{b}_j^m \quad .$$

In the above expressions, C_V^{ℓ} and C_V^{d} are vacancy concentrations in thermal equilibrium with loops and edge dislocations, respectively, when the deviatoric stress is zero. However, both quantities depend on the hydrostatic stress through a multiplicative factor exp $(\sigma_{kk}\Omega/3kT)$.

It is easy to show that the irradiation growth rate tensor $\dot{S}_{ij}$ becomes isotropic only when the loop parameter $N_n R_n$ is the same for all four habit planes, and when the dislocation densities ρ_m for all climb systems are equal. In such a case, there exists no preferred Burgers vector, and $\dot{S}_{ij} \sim \delta_{ij}$. For the following, we shall only treat this case.

§3. IRRADIATION CREEP DUE TO FRANK LOOP GROWTH

The first term in Eq. (23) gives the contribution of the Frank loops to the irradiation creep rate according to SIPA. We shall refer to this contribution as SIPAL creep. For the case of no preferred Burgers vector, we find that

$$\dot{e}^{IC}_{ij} \sim \sum_{n=1}^{4} \hat{b}^n_i \hat{b}^n_j \hat{b}^n_k \hat{b}^n_\ell \tilde{\sigma}_{k\ell} \quad . \tag{24}$$

The sum is most conveniently evaluated in a cartesian coordinate system whose axis coincide with the <100> directions of the cubic lattice. In this coordinate system we denote the deviatoric stress and creep rate tensors as $\tilde{\sigma}^o_{ij}$ and $\dot{e}^o_{ij}$, respectively. The unit Burgers vectors, being normal to the loop habit planes, are listed in Table 1, and the deviatoric stress components normal to the loop planes are given in Table 2. It is then easy to show that

$$\sum_{n=1}^{4} b^n_i b^n_j b^n_k b^n_\ell \tilde{\sigma}^o_{k\ell} = \frac{4}{9} \begin{pmatrix} 0 & 2\sigma^o_{12} & 2\sigma^o_{31} \\ 2\sigma^o_{12} & 0 & 2\sigma^o_{23} \\ 2\sigma^o_{31} & 2\sigma^o_{23} & 0 \end{pmatrix} \tag{25}$$

Table 1

Unit Burgers Vectors for Frank Loops

in a fcc Lattice

n	1	2	3	4
$\sqrt{3}\ \hat{b}^n_1$	1	-1	1	1
$\sqrt{3}\ \hat{b}^n_2$	1	1	-1	1
$\sqrt{3}\ \hat{b}^n_3$	1	1	1	-1

Table 2

The Deviatoric Stress Component

$\hat{b}_k \hat{b}_\ell \tilde{\sigma}^o_{k\ell}$ for Frank Loops

Habit plane index, n	1	2	3	4
$\frac{3}{2}\ \hat{b}^n_k \hat{b}^n_\ell \tilde{\sigma}_{k\ell}$	$\sigma^o_{12}+\sigma^o_{23}+\sigma^o_{31}$	$-\sigma^o_{12}+\sigma^o_{23}-\sigma^o_{31}$	$-\sigma^o_{12}-\sigma^o_{23}+\sigma^o_{31}$	$\sigma^o_{12}-\sigma^o_{23}-\sigma^o_{31}$

We may write this tensor in the more condensed form as

$$\frac{4}{9}(\delta_{ik}\delta_{j\ell} + \delta_{i\ell}\delta_{jk} - 2\delta_{ijk\ell})\tilde{\sigma}^{o}_{k\ell} \quad ,$$

where $\delta_{ijk\ell}$ is a generalized Kronecker tensor whose components are equal to one when all four indices are the same, and zero otherwise.

The irradiation creep law for the SIPAL mechanism can then be written as

$$\dot{e}^{o}_{ij} = \psi^{o}_{ijk\ell}\,\tilde{\sigma}^{o}_{k\ell} \quad , \tag{26}$$

where the creep compliance tensor in the crystal frame is given by

$$\psi^{o}_{ijk\ell} = \psi_2(\delta_{ik}\delta_{j\ell} + \delta_{i\ell}\delta_{jk} - 2\delta_{ijk\ell}) \quad . \tag{27}$$

ψ_2 is a scalar function of the irradiation conditions, the temperature, and the loop density and radius. Its explicit form is of no interest for the present purpose.

§4. IRRADIATION CREEP DUE TO THE CLIMB OF EDGE DISLOCATIONS

This contribution to irradiation creep is given by the second term in Eq. (23), and it will be referred to as SIPAD creep. Again, assuming no preferred Burgers vector, we obtain

$$\dot{e}^{o}_{ij} \sim \sum_{m=1}^{12} \int d\omega_{\ell}\, \delta(\hat{\underset{\sim}{\ell}} \cdot \hat{\underset{\sim}{b}}^{m})[2\hat{b}^{m}_{k}\hat{b}^{m}_{\ell} - (1-4\nu)\,\hat{\ell}_{k}\hat{\ell}_{\ell}]\tilde{\sigma}^{o}_{k\ell}\hat{b}^{m}_{i}\hat{b}^{m}_{j} \tag{28}$$

To carry out the integration over all line directions perpendicular to a given Burgers vector $\underset{\sim}{b}^{m}$, we consider a coordinate system whose z-axis coincides with $\underset{\sim}{b}^{m}$. The line vector $\hat{\underset{\sim}{\ell}}'$ in this coordinate system has the components $(\cos\phi, \sin\phi, 0)$, where ϕ is the azimuthal angle, and

is related to the line vector $\hat{\underset{\sim}{\ell}}$ in the crystal frame by the orthogonal transformation

$$\hat{\ell}_k = a_{kp}\, \hat{\ell}'_p \quad . \tag{29}$$

Hence,

$$\int d\omega_\ell\, \delta(\hat{\underset{\sim}{\ell}} \cdot \hat{\underset{\sim}{b}})\, \hat{\ell}_k\, \hat{\ell}_\ell\, \tilde{\sigma}^o_{k\ell} = a_{kp}\, a_{\ell q}\, \tilde{\sigma}^o_{k\ell}\, \frac{1}{2\pi} \int d\phi\, \hat{\ell}'_p\, \hat{\ell}'_q$$

$$= a_{kp}\, a_{\ell q}\, \tilde{\sigma}^o_{k\ell}\, \frac{1}{2}\, (\delta_{pr}\, \delta_{qr} - \delta_{p3}\, \delta_{q3}) = -\frac{1}{2}\, a_{k3}\, a_{\ell 3}\, \tilde{\sigma}^o_{k\ell} \quad .$$

The coefficients a_{k3} are the directional cosines of the unit Burgers vector $\hat{\underset{\sim}{b}}$ in the crystal frame, i.e., $a_{k3} = \hat{b}_k$. Therefore, we obtain instead of the relation (28)

$$\dot{e}^o_{ij} \sim \frac{1}{2}\, (5-4\nu) \sum_{m=1}^{12} \hat{b}^m_i\, \hat{b}^m_j\, \hat{b}^m_k\, \hat{b}^m_\ell\, \tilde{\sigma}^o_{k\ell} \tag{30}$$

In a fcc lattice the unit Burgers vectors for edge dislocations are those six given in Table 3 plus six more of opposite directions. The deviatoric stress components normal to the climb planes are listed in Table 4, to which must be added six more of opposite sign. With these components, the sum in Eq. (30) can be evaluated easily, and we obtain

$$\sum_{m=1}^{12} \hat{b}^m_i\, \hat{b}^m_j\, \hat{b}^m_k\, \hat{b}^m_\ell\, \tilde{\sigma}^o_{k\ell} = \frac{1}{2} \begin{pmatrix} \tilde{\sigma}^o_{11} & 2\tilde{\sigma}^o_{12} & 2\tilde{\sigma}^o_{13} \\ 2\tilde{\sigma}^o_{12} & \tilde{\sigma}^o_{22} & 2\tilde{\sigma}^o_{23} \\ 2\tilde{\sigma}^o_{13} & 2\tilde{\sigma}^o_{23} & \tilde{\sigma}^o_{33} \end{pmatrix} \quad .$$

Table 3
Unit Burgers Vector for
Edge Dislocations in a fcc Lattice

m	1	2	3	4	5	6
$\sqrt{2}\ \hat{b}_1^m$	1	1	0	-1	-1	0
$\sqrt{2}\ \hat{b}_2^m$	1	0	1	1	0	-1
$\sqrt{2}\ \hat{b}_3^m$	0	1	1	0	1	1

Table 4
The Deviatoric Stress Components
$\hat{b}_k\ \hat{b}_\ell\ \tilde{\sigma}^o_{k\ell}$ for Edge Dislocations

Burgers Vector Index m	$2\hat{b}_k^m\ \hat{b}_\ell^m\ \tilde{\sigma}^o_{k\ell}$
1	$2\tilde{\sigma}^o_{12} - \tilde{\sigma}^o_{33}$
2	$2\tilde{\sigma}^o_{31} - \tilde{\sigma}^o_{22}$
3	$2\tilde{\sigma}^o_{23} - \tilde{\sigma}^o_{11}$
4	$-2\tilde{\sigma}^o_{12} - \tilde{\sigma}^o_{33}$
5	$-2\tilde{\sigma}^o_{31} - \tilde{\sigma}^o_{22}$
6	$-2\tilde{\sigma}^o_{23} - \tilde{\sigma}^o_{11}$

As in the case of SIPAL creep, we can write the creep law in the form of Eq. (26), where the creep compliance tensor for SIPAD creep is now

$$\psi^{o}_{ijk\ell} = \psi_1(\delta_{ik}\delta_{j\ell} + \delta_{i\ell}\delta_{jk} - \delta_{ijk\ell}) \quad , \tag{31}$$

and ψ_1 is a scalar function which depends, among other parameters, on the edge dislocation density.

§5. IRRADIATION CREEP BY CLIMB-CONTROLLED GLIDE

The glide motion of a dislocation with Burgers vector $\underset{\sim}{b}$ produces a strain rate contribution of

$$\frac{1}{2}(b_i\dot{A}_j + b_j\dot{A}_i) \quad ,$$

where the vector $\dot{\underset{\sim}{A}}$ is perpendicular to the glide plane and equal in magnitude to the area swept out per unit time. If there are ρ_d dislocations per unit area belonging to the slip system with index "d", then the total strain rate is given by

$$\dot{e}^{o}_{ij} = \frac{1}{2}\sum_d (b^d_i\dot{A}^d_j + b^d_j\dot{A}^d_i)\rho_d \quad . \tag{32}$$

It is now assumed that the rate of slip is determined by the rate of escape from obstacles for trapped edge dislocations. The waiting time at obstacles is supposed to be much larger than the transit time between consecutive stops. Let v_d be the average climb velocity, h_d the average obstacle height, and L_d the average glide distance perpendicular to the line vector $\hat{\underset{\sim}{\ell}}$. Then

$$\dot{A}_i = \hat{g}_i L_d \upsilon_d / h_d \quad ,$$

where $\hat{\underset{\sim}{g}}$ is a unit vector normal to the glide plane.

The strain rate tensor is then given by

$$\dot{e}^o_{ij} = \frac{1}{2} \sum_d \rho_d (L_d \upsilon_d / h_d) \, (b^d_i \hat{g}^d_j + b^d_j \hat{g}^d_i) \quad . \tag{33}$$

To obtain the stress dependence for the CCG creep we must first specify the stress dependence of $\rho_d L_d \upsilon_d / h_d$. During irradiation, and particularly when void growth occurs, dislocations climb without the assistance of the external stress. We may then assume that the climb velocity υ_d is independent of the stress and the glide system. Furthermore, we may also rule out the possibility for dislocation multiplication by the deformation process when the stress is sufficiently below the yield point; ρ_d will then also be the same for all glide systems and independent of the stress. The stress dependency must then arise from the ratio L_d/h_d.

We assume, as Gittus (1972) did, that L_d/h_d is proportional to the shear stress τ_d acting in the glide plane in the direction of the Burgers vector $\underset{\sim}{b}^d$. Accordingly,

$$L_d/h_d = \kappa \, \tau_d / \mu \tag{34}$$

where κ is a constant, μ the shear modulus, and

$$\tau_d = \hat{b}^d_k \, \sigma^o_{k\ell} \, \hat{g}^d_\ell \quad . \tag{35}$$

In order to ensure that positive work is done by the external stress for slip on each system, it is convenient to introduce the creep dissipation function

Table 5

Glide Systems in the fcc Lattice

Glide System Index, d	1,2,3	4,5,6	7,8,9	10,11,12
Glide Plane	(111)	$(\bar{1}\bar{1}1)$	$(\bar{1}11)$	$(1\bar{1}1)$
Burgers Vectors	$[01\bar{1}]$ $[\bar{1}01]$ $[1\bar{1}0]$	$[0\bar{1}\bar{1}]$ $[101]$ $[\bar{1}10]$	$[01\bar{1}]$ $[101]$ $[\bar{1}\bar{1}0]$	$[0\bar{1}\bar{1}]$ $[\bar{1}01]$ $[110]$

Table 6

Shear Stress τ_d for the Glide Systems of the fcc Lattice*

Glide System	τ_d	Glide System	τ_d	Glide System	τ_d
1	$\sigma_{22}-\sigma_{33}+\sigma_{12}-\sigma_{13}$	2	$\sigma_{33}-\sigma_{11}-\sigma_{12}+\sigma_{23}$	3	$\sigma_{11}-\sigma_{22}+\sigma_{13}-\sigma_{23}$
4	$\sigma_{22}-\sigma_{33}+\sigma_{12}+\sigma_{13}$	5	$\sigma_{33}-\sigma_{11}-\sigma_{12}-\sigma_{23}$	6	$\sigma_{11}-\sigma_{22}-\sigma_{13}+\sigma_{23}$
7	$\sigma_{22}-\sigma_{33}-\sigma_{12}+\sigma_{13}$	8	$\sigma_{33}-\sigma_{11}+\sigma_{12}+\sigma_{23}$	9	$\sigma_{11}-\sigma_{22}-\sigma_{13}-\sigma_{23}$
10	$\sigma_{22}-\sigma_{33}-\sigma_{12}-\sigma_{13}$	11	$\sigma_{33}-\sigma_{11}+\sigma_{12}-\sigma_{23}$	12	$\sigma_{11}-\sigma_{22}+\sigma_{13}+\sigma_{23}$

*For the sake of clarity the superscript "o" is omitted.

$$\dot{\phi} = \frac{1}{2}\,\dot{e}_{ij}\,\sigma_{ij} = \frac{1}{2}\,(\kappa\rho v/\mu b)\sum_{d}\,[b_i^d \hat{g}_j^d \sigma_{ij}^o]^2 \tag{36}$$

from which one can recover the creep law by differentiation:

$$e_{ij}^o = \frac{1}{2}\,[\partial\dot{\phi}/\partial\sigma_{ij}^o + \partial\dot{\phi}/\partial\sigma_{ji}^o] \quad . \tag{37}$$

It is straightforward to evaluate for all the glide systems listed in Table 5 the corresponding shear stresses τ_d. The sum of all τ_d^2 is then proportional to the creep dissipation function $\dot{\phi}$. For the derivatives of $\dot{\phi}$ one finds

$$\partial\dot{\phi}/\partial\sigma_{11}^o \sim 2\sigma_{11}^o - \sigma_{22}^o - \sigma_{33}^o = 3\tilde{\sigma}_{11}^o \quad , \tag{38}$$

$$\partial\dot{\phi}/\partial\sigma_{12}^o \sim 2\sigma_{12}^o = 2\tilde{\sigma}_{12}^o \quad , \tag{39}$$

and analogous expressions for the other ones.

Again, the constitutive law for CCG-creep can be written in the form of Eq. (26), where the creep compliance tensor is now given by

$$\psi_{ijk\ell}^o = \psi_{-1}\,(\delta_{ik}\delta_{j\ell} + \delta_{i\ell}\delta_{jk} + \delta_{ijk\ell}) \quad . \tag{40}$$

Here, ψ_{-1} is a scalar function which depends on the dislocation density, the climb velocity, and other parameters.

§6. THE GENERAL CONSTITUTIVE LAW

Upon comparing the Eqs. (27), (31), and (40), it is evident that the total creep compliance tensor with contributions from all three mechanisms can be written in the compact form

$$\psi_{ijk\ell}^o = \sum_{\eta=-1}^{2}{}' \psi_\eta[\delta_{ik}\delta_{j\ell} + \delta_{i\ell}\delta_{jk} - \eta\delta_{ijk\ell}] \quad , \tag{41}$$

where the index η is defined as

$$\eta = \begin{cases} 2 & \text{for SIPAL creep} \\ 1 & \text{for SIPAD creep} \\ -1 & \text{for CCG creep.} \end{cases} \tag{42}$$

For an arbitrary coordinate system, called the specimen frame, obtained by the orthogonal transformation

$$x_i = a_{ij} x_j^o \tag{43}$$

of the crystal frame, the constitutive law is given by

$$\dot{e}_{ij} = \psi_{ijk\ell}\, \tilde{\sigma}_{k\ell} \quad , \tag{44}$$

where both the creep strain rate $\dot{e}_{ij}$ and the deviatoric stress $\tilde{\sigma}_{k\ell}$ are now specified in the specimen frame, and where

$$\psi_{ijk\ell} = \sum_{\eta} \psi_{\eta} \left(\delta_{ik}\delta_{j\ell} + \delta_{i\ell}\delta_{jk} - \eta \sum_{n=1}^{3} a_{in}a_{jn}a_{kn}a_{\ell n}\right) . \tag{45}$$

Eqs. (44) and (45) represent the general constitutive law for irradiation creep in fcc single crystals with a dislocation structure having no preferred Burgers vector.

The creep compliance tensor is rendered anisotropic because of the terms proportional to η, and since η is different for the three mechanisms considered, each mechanism gives rise to a distinct character of the anisotropy. Therefore, by measuring this anisotropy, it should be possible to determine the dominant irradiation creep mechanism.

§7. TWO EXAMPLES

In order to demonstrate the anisotropy of irradiation creep, we illustrate this by considering the two cases of uniaxial tension, and of torsion of a bar specimen.

Let the axis of this specimen be the x_3 - axis of our specimen frame. We may imagine that this frame is obtained from the crystal frame by two rotations as indicated in Fig. 1. The specimen orientation is then specified by the two rotation angles Θ and ϕ which also correspond to a certain point on the stereographic triangle onto which we shall map the points of equal creep rate.

The transformation matrix connecting crystal to specimen frame is given by

$$a_{ij} = \begin{pmatrix} \cos\Theta\cos\phi & \cos\Theta\sin\phi & \sin\Theta \\ -\sin\phi & \cos\phi & 0 \\ -\sin\Theta\cos\phi & -\sin\Theta\sin\phi & \cos\Theta \end{pmatrix}$$

and its elements are to be inserted in Eq. (45).

For uniaxial tension all stresses are zero except $\sigma_{33} = \sigma$. The axial creep rate $\dot{e} = \dot{e}_{33}$ according to Eq. (44) becomes

$$e = \frac{1}{3}\,(2\psi_{3333} - \psi_{3311} - \psi_{3322})\,\sigma \quad .$$

Considering only one creep mechanism at a time, we obtain the following relationship:

$$3\dot{e}/\psi_\eta\sigma = 4 - 2\eta\,(F\sin^4\Theta + \cos^4\Theta) + \eta\sin^2\Theta\,[1 - F + 2(1+F)\cos^2\Theta], \quad (46)$$

where

$$F = \sin^4\phi + \cos^4\phi \quad . \tag{47}$$

This normalized creep rate is shown in Figs. 2, 3, and 4 for the SIPAL, SIPAD, and CCG mechanism, respectively. We note that in the case of SIPAL creep no deformation occurs for tension in the <001> directions. Also, the SIPAD mechanism gives the least, and the CCG mechanism the most creep for these directions. On the other hand, for tension in the <111> directions the SIPA mechanisms exhibit a maximum, and the CCG mechanism shows a minimum creep rate.

In the case of torsion around the x_3-axis the state of stress is given by

$$\sigma_{13} = -\mu\alpha_e x_2 \quad , \quad \sigma_{23} = \mu\alpha_e x_1 \, , \tag{48}$$

and all the other components are zero. Here, α_e is the twist angle per unit length of the specimen due to the elastic deformation. The rate of change of this twist angle due to creep is given by an integration over the cross-section:

$$\dot{\alpha} = \frac{1}{J} \int dA \, (\dot{e}_{23} x_1 - \dot{e}_{13} x_2) \, . \tag{49}$$

J is the torsional rigidity. Using the constitutive law and the stresses of Eq. (48) we obtain the relationship

$$\dot{\alpha} = (\psi_{2323} + \psi_{1313}) \, 2\mu \, \alpha_e \tag{50}$$

For a specific creep mechanism this equation yields the expression

$$\dot{\alpha}/\mu\alpha_e = 4 - 2\eta \sin^2\theta [1 - F \sin^2\theta + \cos^2\theta] \, , \tag{51}$$

which is shown in Figs. 5, 6, and 7 for the SIPAL, SIPAD, and CCG mechanism, respectively.

In opposition to uniaxial tension, the SIPA mechanisms give the most creep for torsion around the <001> directions, and the least for the <111> directions. However, this is reversed for the CCG mechanism.

§8. DISCUSSION

A distinction between the SIPA mechanisms and the CCG mechanism can clearly be made with the proposed experiments on single crystals if all mechanisms do not contribute equally to irradiation creep. In a recent comparison (Wolfer 1979) between the experimental results and theoretical predictions, it was found that the SIPA mechanism is not sufficient to account for the measured irradiation creep strains in pressurized tubes of type 316 stainless steel irradiated to a fluence of less than about $2-3 \times 10^{26}$ n/m^2. However, above this fluence value, SIPA creep accounts for most of the irradiation creep strain. This fluence value also coincides with the dose at which the network dislocation density has reached saturation in solution annealed type 316 stainless steel.

It appears then that irradiation creep at low doses proceeds mainly via the CCG mechanism or possibly similar glide mechanisms. In order to test for the SIPA mechanisms, it would be necessary to pre-irradiate the single crystal specimens to a sufficiently large dose. This dose limit depends on the material as well as on the irradiation temperature. For low irradiation temperatures, a high density of loops is reached after relatively low doses. In materials with low stacking fault energies, irradiation creep is then expected to proceed via the SIPAL mechanism. On the other

hand, at high irradiation temperatures the dislocation loop density remains low, and irradiation creep at high doses is expected to be due to a combination of SIPAD and CCG creep. In this case, we anticipate a less distinctive orientation dependence of irradiation creep.

ACKNOWLEDGEMENT

This work was supported by the Division of Basic Energy Sciences, U.S. Department of Energy, under contract ER-78-S-02-4861 with the University of Wisconsin.

REFERENCES

Bloom, E.E., and Wolfer, W.G., 1978, ASTM STP 683.

Gilbert, E.R., Straalsund, J.L., and Wire, G.L., 1977, J. Nucl. Materials, 65, 266.

Gittus, J.H., 1972, Phil. Mag. 25, 345.

Harris, D.R., 1977, J. Nucl. Materials, 65, 157.

Heald, P.T., and Speight, M.V., 1974, Phil. Mag., 29, 1075.

Nabarro, F.R.N., 1967, Phil. Mag., 16, 231.

Wolfer, W.G., Ashkin, M., and Boltax, A., 1976, ASTM STP 570, P. 233.

Wolfer, W.G., and Ashkin, M., 1975, J. Appl. Phys., 46, 547; 1976, Ibid., 47, 791.

Wolfer, W.G., and Boltax, A., 1973, European Conf. on Irradiation Embrittlement and Creep in Fuel Cladding and Core Components, London, Nov., 1972, Paper 31.

Wolfer, W.G., 1978, ASTM STP 683.

Wolfer, W.G., 1979, Internat. Conf. on Fund. Mechanisms of Radiation-Induced Creep and Growth, Chalk River, Canada, May 1969; to be published in J. Nucl. Materials.

List of Figures

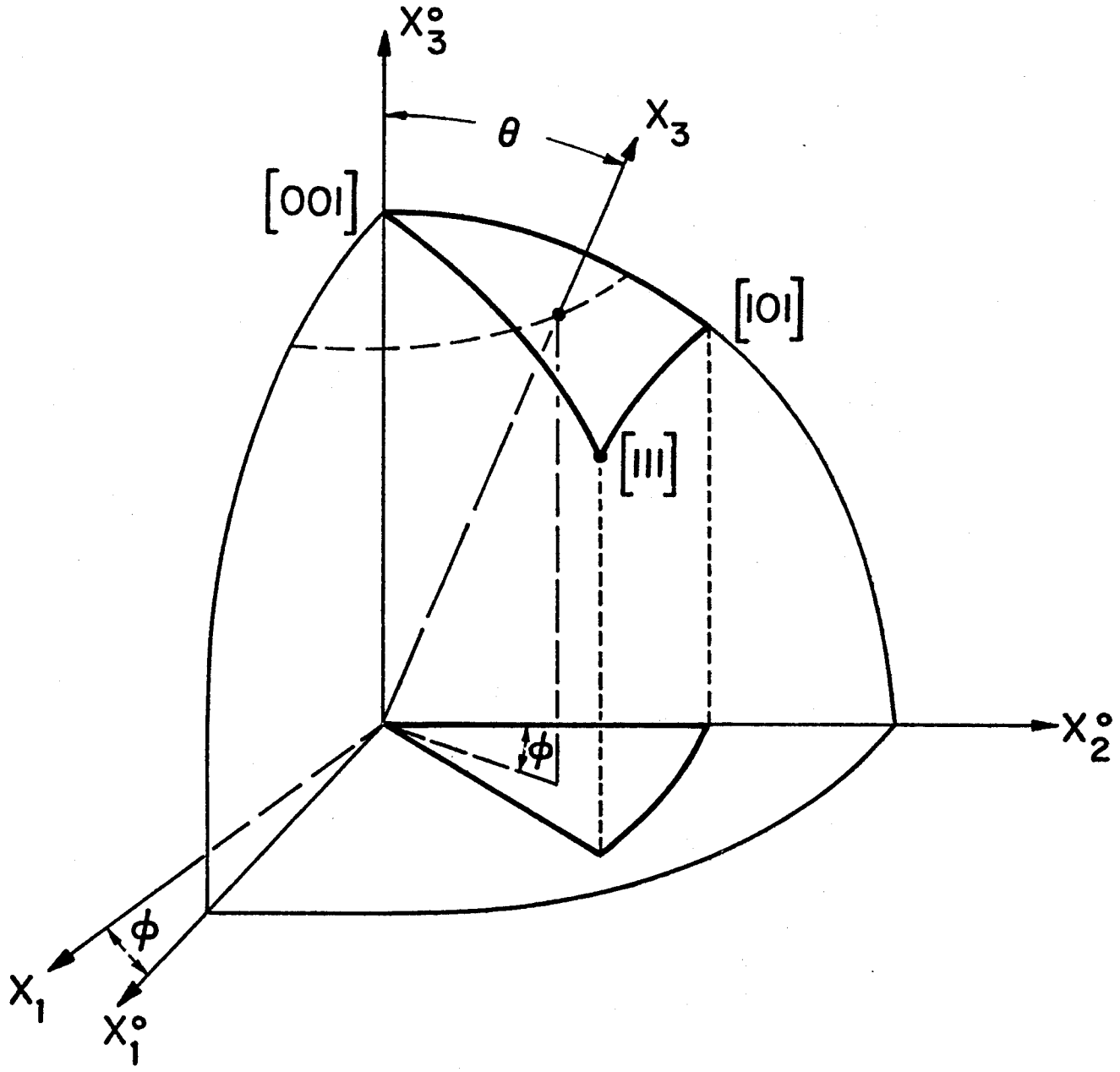

Fig. 1. The relation between the crystal (x_i^o) and the specimen (x_i) coordinate system.

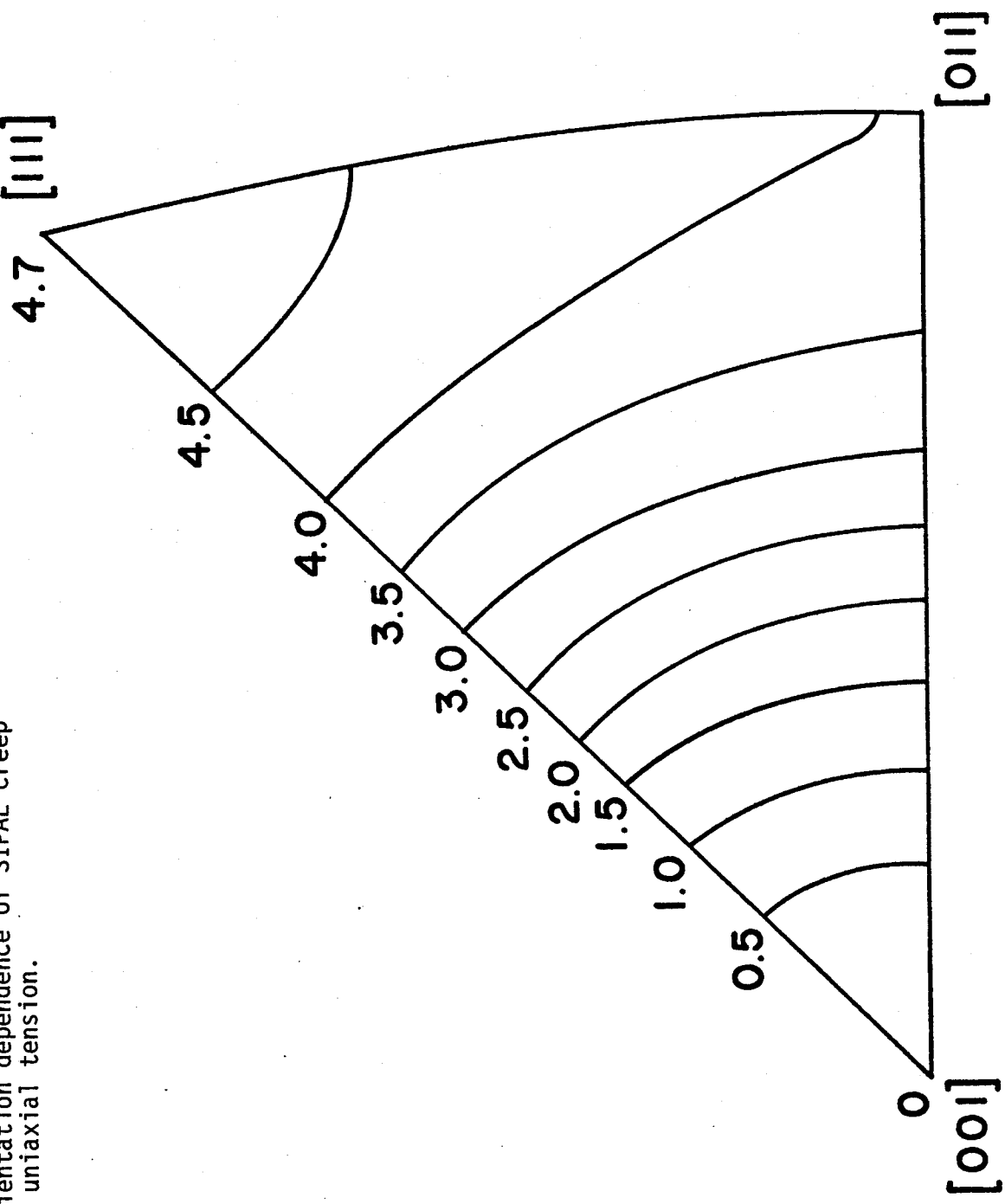

Fig. 2. Orientation dependence of SIPAL creep in uniaxial tension.

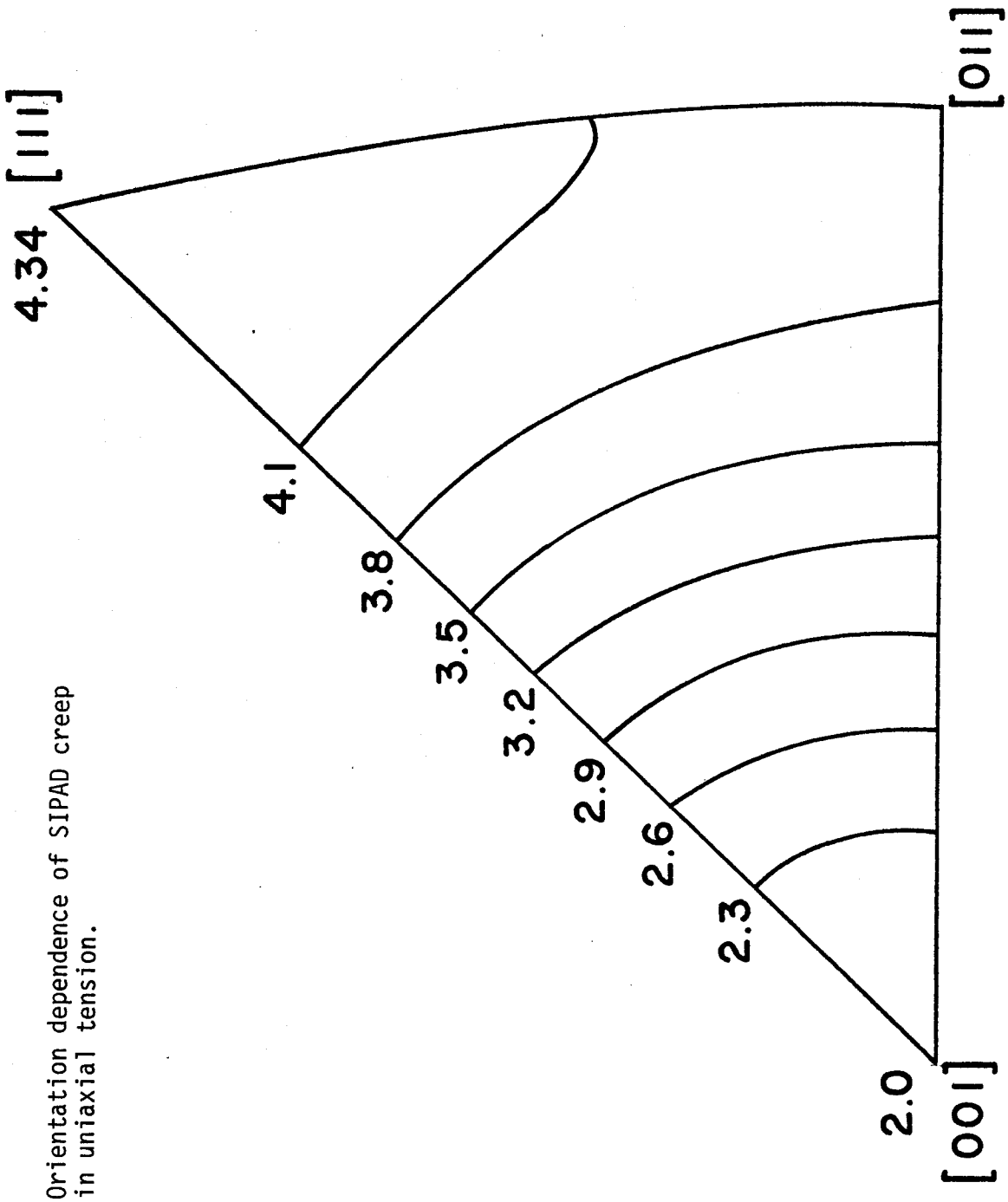

Fig. 3. Orientation dependence of SIPAD creep in uniaxial tension.

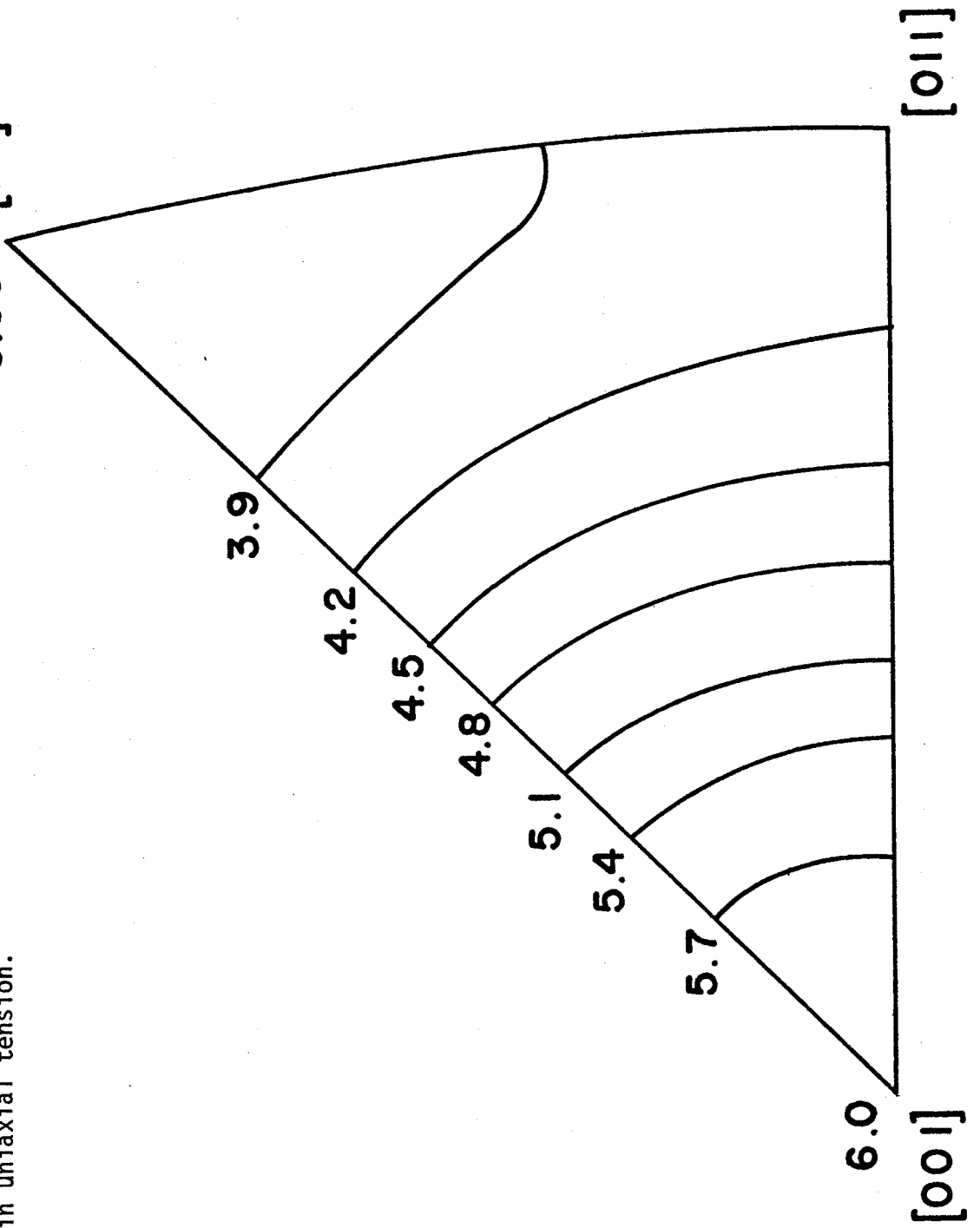

Fig. 4. Orientation dependence of CCG creep in uniaxial tension.

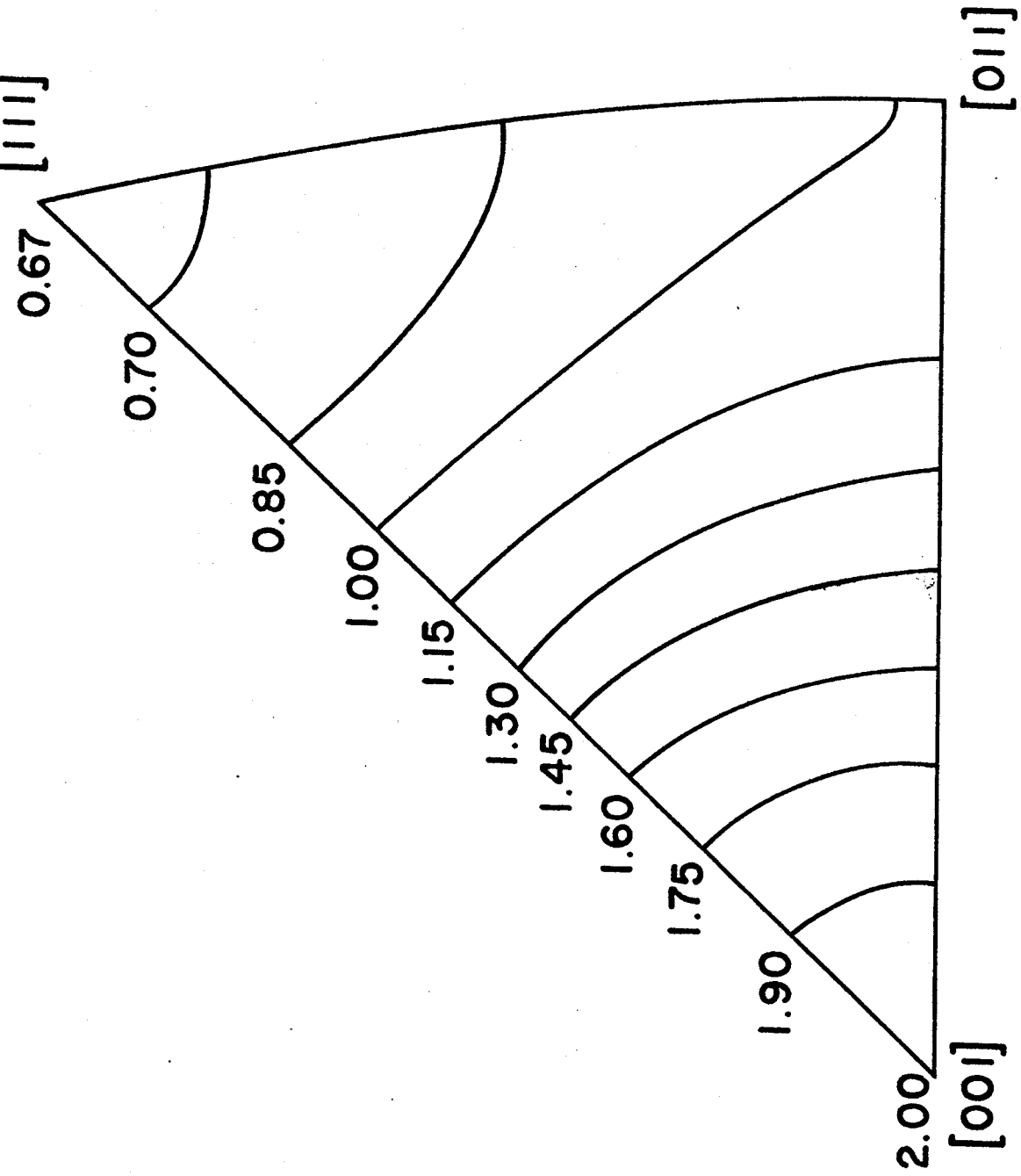

Fig. 5. Orientation dependence of SIPAL creep in torsion.

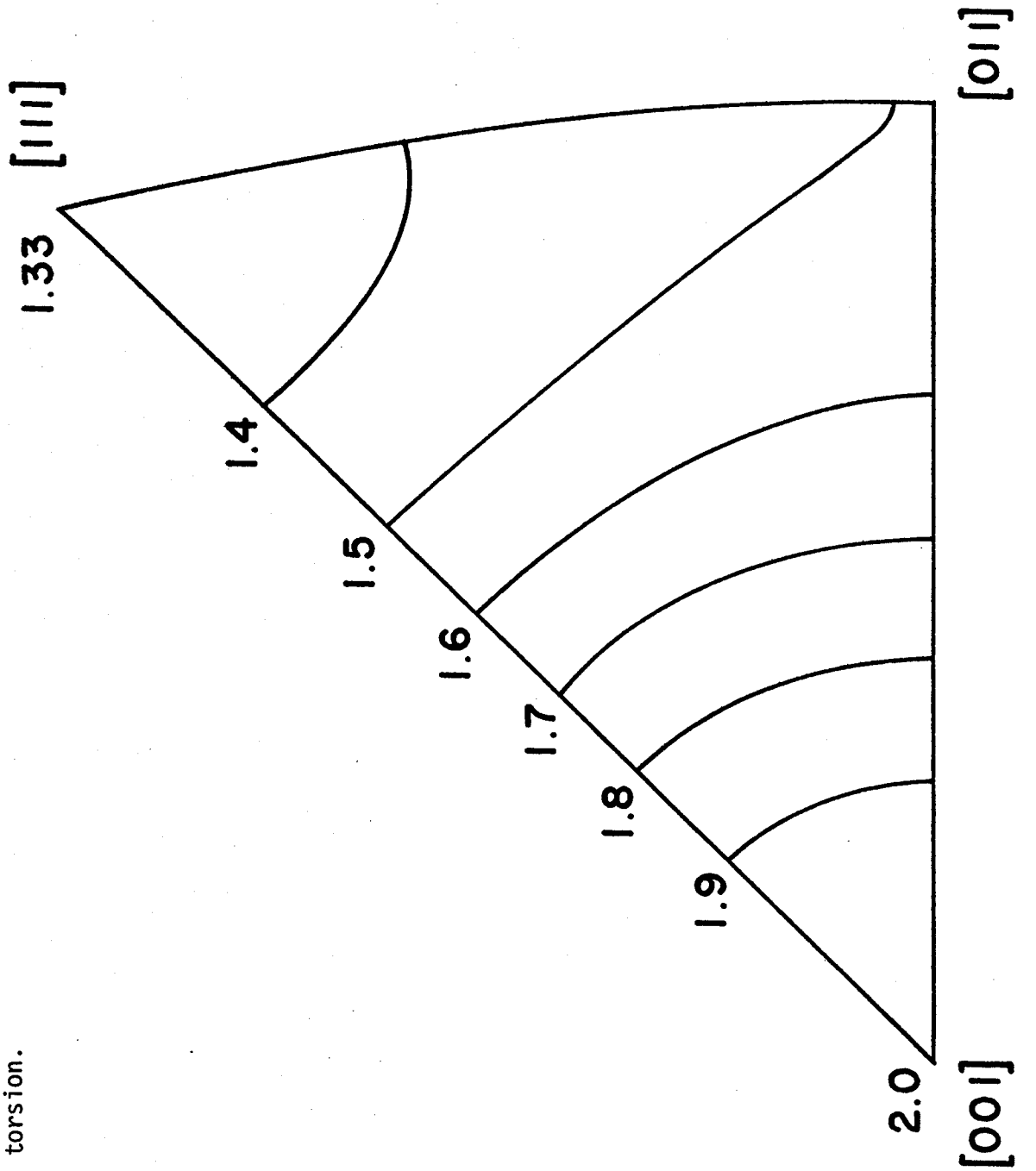

Fig. 6. Orientation dependence of SIPAD creep in torsion.

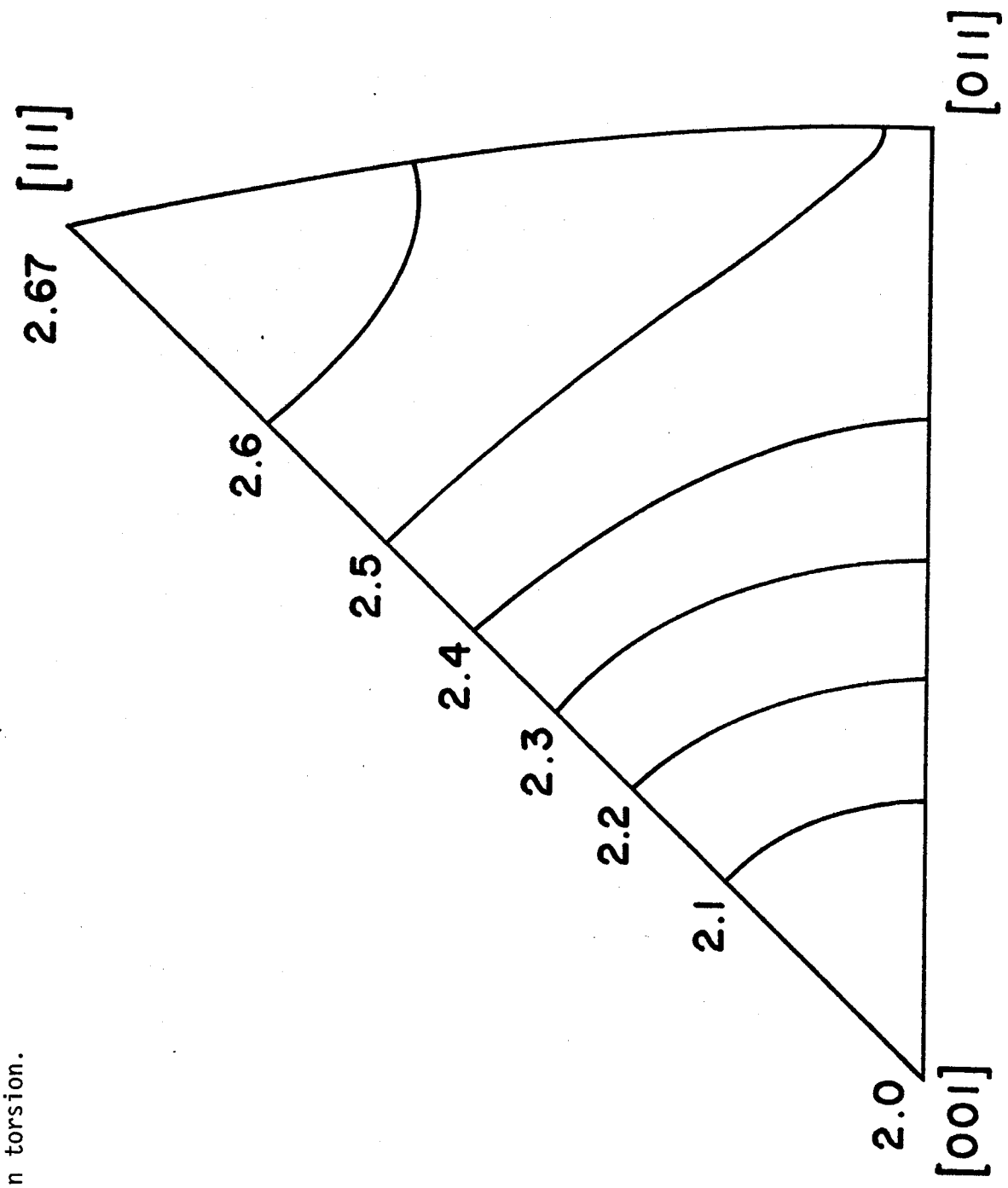

Fig. 7. Orientation dependence of CCG creep in torsion.